Ising-like dynamical signatures and the end point of the QCD transition line

Sz. Borsányi,* A. Patkós,† D. Sexty,‡ and Zs. Szép§
Department of Atomic Physics, Eötvös University, H-1117 Budapest, Hungary
(Received 31 May 2001; published 27 November 2001)

An increase in the size of coherent domains in the one component Φ^4 field theory under the influence of a uniformly changing external magnetic field near the critical end point $T_\Phi = T_c, h_\Phi = 0$ was proposed recently as an estimate also for the variation of the chiral correlation length of QCD near its respective hypothetical end point in the T_{QCD}-μ_{QCD} plane. The present detailed numerical investigation of the effective model suggests that passing by the critical QCD end point with a realistic rate of temperature change will trigger large amplitude oscillations in the temporal variation of the chiral correlation length. A simple mechanism for producing this phenomenon is suggested.

DOI: 10.1103/PhysRevD.64.125011 PACS number(s): 11.10.Wx

I. INTRODUCTION

The quality of our knowledge of the phase structure of QCD at high temperature and finite baryon density is an important benchmark for our understanding of strong interactions. A critical end point of the first order phase transition line in the T-μ projection of the QCD phase diagram was conjectured [1] to follow from the compatibility of the following observations.

(i) Lattice simulations [2] indicate that the phase transformation at zero chemical potential with realistic quark masses is a crossover, characterized by an analytic variation of the thermodynamical potential with the temperature.

(ii) At zero temperature there is a first order phase transition from the hadron phase to more exotic phases as a function of μ [3] which continues as a first order line into the (T,μ) plane.

For the strong matter the significance of this end point would be similar to that of the Curie point for ferromagnets.

Recently, some important progress was realized in the search for the (μ_E, T_E) location of the end point with nonperturbative lattice studies [4]. There is a chance in current heavy ion collision experiments that it can be observed experimentally, since with increasing collision energy per nucleon the central rapidity particle spectra explore regions of the phase diagram corresponding to a decreasing chemical potential. An obvious class of the signatures would reflect the increasing size of the coherent fluctuations in the order parameter σ field in the neighborhood of the end point [5]. In this region mostly the σ field will be excited, since its mass is the lightest near the critical end point in view of the amount of explicit chiral symmetry breaking which keeps the pions massive. This coherence should be reflected by the statistics of the main decay products of the σ field, the pions.

Starting from equilibrium at some $T_0 > T_c$, and passing with finite velocity near the end point, the system unavoidably slows out of equilibrium. In contrast with the equilibrium characterization of the second order transition, a finite maximal correlation length is reached with a certain amount of supercooling. A substantial increase in the correlation length will be a reliable signal for the existence of the critical end point.

Quantitative predictions for this phenomenon should rely on nonequilibrium field theory. For the moment it is hopeless to simulate directly the far from equilibrium behavior of QCD matter. One recognizes however, that the mass of the σ in this region is separated by a gap from the other mesonic excitations. Therefore, one arrives at the conclusion that an effective dynamical theory of the longest wavelength excitations in this region is in the same universality class as the Ising model. At present no quantitative matching is known between the original theory and its one-component Φ^4 effective version. Still, universal features of the class A of critical dynamics (in the classification of Hohenberg and Halperin [6]) are expected to occur.[1]

Recently Berdnikov and Rajagopal (BR) [7] proposed an intuitive mapping. They approximately identify the magnetic field (h) of the Ising model with the temperature of the QCD [the Ising reduced temperature (r) axis is nearly parallel to the chemical potential axis of QCD]. They checked that the results are not sensitive to a moderate tilt in this mapping. Next, they proposed a dynamical equation which describes the evolution of the inverse correlation length (the mass of the σ meson) when the system passes through the critical end point of the Ising model with finite velocity under different angles. This equation was shown to depend on a single nonuniversal parameter, proportional to the rate of change of the Ising magnetic field.

Finally, a semiquantitative correspondence was proposed between the relevant QCD temperature range ($T_0 = 180$ MeV, $T_{freeze\text{-}out} = 120$ MeV) and the dimensionless strength of the Ising magnetic field ($h_0 = -0.2, h_{final} = 0.1$). The nonuniversal constant was varied in a wide range, since it essentially relates the rate of cooling of the QCD matter to the speed of the variation of the external field h. The main

*Email address: mazsx@cleopatra.elte.hu
†Email address: patkos@ludens.elte.hu
‡Email address: sexty@cleopatra.elte.hu
§Email address: szepzs@cleopatra.elte.hu

[1] A more complete theory reflecting the direct influence of the temporal variation of a conserved baryon number density on the σ field falls into class C [7], and will be the subject of future study.

result of Ref. [7] was a prediction for the variation of the order parameter (e.g. σ) correlation length with the variation of h in the neighborhood of the critical end point.

The variation of the correlation length during passage through the critical point was compared to its value taken at the noncritical starting value, which corresponds to the equilibrium energy density of the QCD plasma produced in the collision ($T=T_0$). It is the relative increase in the correlation length at the freeze-out of the system ($T=T_{freeze\text{-}out}$), where most of the pions are coming from, which is the most important issue. A factor of 2–3 increase was signaled, which is claimed to be observable under the accuracy of the present heavy ion experiments.

The aim of our present investigation is to check the accuracy of the first order relaxational dynamics assumed for the inverse correlation length. For this we have integrated exactly the equations of motion of the one-component classical three-dimensional scalar field $\Phi_d(\mathbf{x},t)$ on lattices of size $N=16$–128:

$$\ddot{\Phi}_d(\mathbf{x},t)=(\Delta-m^2)\Phi_d(\mathbf{x},t)-\frac{\lambda}{6}\Phi_d^3(\mathbf{x},t)-h_d(t), \qquad (1)$$

and measured simultaneously the variation of the order parameter and of the correlation length.

Although the hadronic system freezes out at $T_{freeze\text{-}out}\sim 120$ MeV, which corresponds to $h=0.1$ in the effective system, we have followed the variation of the correlation length and of the order parameter to higher values of h. This enabled us to recognize the relevance of a second order dynamics in the effective equation of motion of these characteristics.

It turns out that the order parameter (OP) obeys an equation which is slightly more complicated than the one proposed by Halperin and Hohenberg for this class. It is formally analogous to the differential equation of a damped oscillator. In order to achieve good quantitative description of the OP trajectory obtained from the numerical simulations, one has to take into account the effect of slowing out from equilibrium while the system passes by the critical point.

Our paper is organized in the following way. In Sec. II the method of numerical solution of Eq. (1) is briefly outlined. The methods of analyzing the time evolution of the system are presented in more detail with special emphasis on the determination of the spatial correlation length. In Sec. III the trajectories of the most important quantities characterizing the state of the system are mapped out in the (r,h) and the (OP,h) planes when passing at different distances by the critical Ising end point. In Sec. IV we present the results for the nonequilibrium h evolution of the correlation length for several values of $a^{-1}\equiv dh/dt$ and compare them with the estimates of BR. Finally, in Sec. V a quantitative phenomenological interpretation of the measured order parameter trajectory is offered. Our dynamical description is compared to the equation of motion proposed for this class by Halperin and Hohenberg. Based on the proposed effective relaxational dynamics we suggest also a simple way to account for the variation of the correlation length. Conclusions of our investigation are summarized in Sec. VI.

II. METHODS OF SOLVING AND ANALYZING THE EXACT CLASSICAL EQUATIONS

For setting up and numerically solving the Φ^4 theory we used techniques similar to those applied in our previous paper [8]. Here we briefly outline the procedure.

As a first step one has to rewrite Eq. (1) using dimensionless quantities (not having index d), defined as follows:

$$t=t_d/a_x, \quad x=x_d/a_x,$$

$$\Phi=\sqrt{\frac{\lambda}{6}}a_x\Phi_d, \quad h=\sqrt{\frac{\lambda}{6}}a_x^3 h_d, \qquad (2)$$

where a_x stands for the lattice spacing, the powers of which we used to scale dimensionful quantities. The dimensionless mass parameter of the theory $|m|=a_x|m_d|$ was set to unity. The field equation in dimensionless variables is of the following form:

$$\Phi_{\mathbf{n}}(t+a_t)+\Phi_{\mathbf{n}}(t-a_t)-2\Phi_{\mathbf{n}}(t)-a_t^2/a_x^2\sum_i [\Phi_{\mathbf{n}+\hat{\mathbf{i}}}(t) + \Phi_{\mathbf{n}-\hat{\mathbf{i}}}(t)-2\Phi_{\mathbf{n}}(t)]+a_t^2[-\Phi_{\mathbf{n}}+\Phi_{\mathbf{n}}^3-h(t)]=0. \qquad (3)$$

There were a number of simple quantities routinely monitored in each run. The first was twice the average kinetic energy per site (also called the kinetic temperature for nonequilibrium field configurations):

$$T_{kin}(t)=\frac{1}{L^3}\sum_{\mathbf{n}}\dot{\Phi}_{\mathbf{n}}^2(t); \qquad (4)$$

the second, the trajectory of the homogeneous (OP) mode:

$$\bar{\Phi}(t)=\frac{1}{L^3}\sum_{\mathbf{n}}\Phi_{\mathbf{n}}(t)\equiv\overline{\Phi(x,t)}^V. \qquad (5)$$

Its fluctuation

$$\delta\Phi^2(t)=\overline{\Phi^2(x,t)}^V-(\overline{\Phi(x,t)}^V)^2 \qquad (6)$$

was also used.

The thermalization algorithm, which led to the initial state, consisted of two steps. First we set the initial energy density by continuously comparing the desired and the measured kinetic temperatures. Depending on the deviation from the targeted temperature an artificial friction or antifriction term was introduced into Eq. (3). After reaching the required kinetic energy density, in a second step the original form of the discretized nonlinear field equation was iterated until thermalization was complete. Both steps were repeated until the final kinetic temperature was just what we desired.

The critical temperature $T_{\Phi,c}$ was determined at $h=0$ by locating on the T_Φ axis the maximum of $\delta\Phi^2$, or of the specific heat, and by finding the point separating zero and nonzero expectation value regions of the OP, $\bar{\Phi}$. The reduced temperature $r\equiv(T_\Phi-T_{\Phi,c})/T_{\Phi,c}$ was measured relative to $T_{\Phi,c}=1.5$ for $L=32$ and $T_{\Phi,c}=1.57$ for $L=64$.

A. Determination of the correlation length

The main goal of this paper is to give a quantitative interpretation of the dynamical behavior of the correlation length as the system passes by the critical end point. Therefore we need an accurate measurement method for this quantity, which is reliable in a dynamical system too.

(1) The most straightforward way is to use the definition of the correlation function:

$$C(\Delta,t)=\langle\overline{\Phi(x,y,z+\Delta,t)\Phi(z,y,z,t)}\rangle-\langle\overline{\Phi}(t)\rangle^2. \quad (7)$$

Here the overbar refers to the spatial average of some quantity at fixed t in a single sample, while the angular brackets stand for the average over the initial conditions. After checking that $C(\Delta,t)$ truly behaves as $\sim\cosh[(\Delta-L/2)/\xi_1]$, one can extract the correlation length ξ_1. We refer to this characteristic length as the ''direct'' length of correlation below.

(2) The average linear size of the regions of the same sign deviations from the space average $\overline{\Phi}$ can be taken to estimate the characteristic size of coherent fluctuations. Consider $\Phi(\mathbf{x},t)-\overline{\Phi}(t)$. At a given time a histogram was constructed by scanning through the lattice for the number of occurrences of site sequences with the same sign deviation from $\overline{\Phi}(t)$, and of a given length Δ, parallel to the lattice axes. The histogram showed perfect exponential dependence on Δ. Its characteristic length defines the ''grain size'' ξ_2. Repeating this measurement for every configuration during the time evolution, one obtains the function $\xi_2(t)$.

The correlation lengths defined by the above algorithms are different, of course. One expects, however, that both definitions capture the same feature of a field configuration and there exist simple functional relationships between them. In order to find the relation of ξ_i to the standard correlation length (or its inverse, the mass), which is usually measured with method 5 (see below), we studied the equilibrium systems at different values of the reduced temperature $r\in(0,0.27)$. Using the algorithms described above one finds the functions $\xi_i(r)$, as well as the standard $m_{eff}(r)$. The elimination of r leads to the relations $m_{eff}=g_i(\xi_i)$, well approximated by second order polynomials. In principle, one should establish this relation for each value of h separately, but in practice the relation found for $h=0$ gave good agreement between the results of the different methods away from equilibrium also.

B. Spectral determination of the mass

An algorithm for the reconstruction of the effective potential from the real time evolution of a scalar field was presented in [8]. An effective equation of motion was fitted to the temporal variation of the order parameter. Its ''force'' term was interpreted as the derivative of the effective potential with respect to the field. Then it was easy to identify the effective squared mass.

This time we further improved this algorithm. All spatial Fourier modes of the system are used for the reconstruction of the dispersion relations. Three stages of the implementation were worked out.

(3) We assumed the validity of the following approximate equation for short time intervals:

$$Z\ddot{\Phi}-\Delta\Phi+m_{eff}^2\Phi+\epsilon\Delta^2\Phi=0, \quad (8)$$

where Δ is understood as lattice discretization to the Laplacian. Comparing this to the real nonlinear evolution we could fit Z,m_{eff}^2,ϵ for the short intervals in question in the following way. A spatial fast Fourier transform (FFT) algorithm was applied to the field configurations generated by Eq. (3). The temporal trajectory of each $\hat{\mathbf{k}}$ mode was fitted to the equation dictated by the Fourier transform of Eq. (8). The coefficients of the polynomial of $\hat{k}^2$ also determine the time dependent effective mass. [Here and in the following $\hat{k}_i=2(\sin k_i/2)$ stands for the dimensionless lattice momentum.] A lower bound for the length of the time interval in which Eq. (8) is fitted comes from the consistency criterion that the time interval we averaged over must be much greater than the resulting $1/m_{eff}$ time scale. For out-of-equilibrium field configurations there is also an upper bound for the time interval which is set by the variation rate of the parameters r,h.

(4) For the two-point function related to the OP susceptibility [9] the relation

$$\frac{T}{\langle|\Phi_{\mathbf{k}}|^2\rangle}=Z^{-1}[m_{eff}^2+\hat{k}^2+\varepsilon\hat{k}^4+\mathcal{O}(\hat{k}^6)] \quad (9)$$

holds in equilibrium [10]. Replacing the ensemble average in the denominator of the left hand side by averaging over the $\mathbf{k}$ modes characterized by equal $\hat{k}^2$ and using $T_{kin,\hat{k}^2}=\overline{|\dot{\Phi}_{\mathbf{k}}|^2}^{\Omega_{\mathbf{k}}}$ for T we found that our system obeys Eq. (9) for $\hat{k}^2>1$ without any time averaging. With these replacements we could fit the value of $m_{eff}^2(h)$ continuously both near and far from equilibrium. The wave function renormalization constant was found to be equal to 1 up to 0.5% in all cases. The coefficient ε of the fourth derivative correction term was checked to be negligible.

(5) Since most of the modes with $\hat{k}^2>1$ nicely follow the above behavior, one might improve the statistical confidence of the above algorithm by summing over the contribution of all modes (including $\hat{k}^2<1$), which yields the approximate equality

$$\frac{\delta\Phi^2}{T}=\frac{1}{L^3}\sum_{\mathbf{k}\neq\mathbf{0}}\frac{1}{m_{eff}^2+\hat{k}^2}, \quad (10)$$

with $\delta\Phi^2$ denoting the field fluctuation as defined in Eq. (6). Its measurement does not require the application of the time consuming FFT. The value of the function on the right hand side can be tabulated and Eq. (10) is quickly solved with help of a look-up table plus interpolation for every measured value of $\delta\Phi^2$.

In addition, as a quick reference the so-called Hartree squared mass estimate $m_{Hartree}^2=-1+3(\overline{\Phi}^2+\delta\Phi^2)$ was also used. It proved useful in interpreting qualitatively the

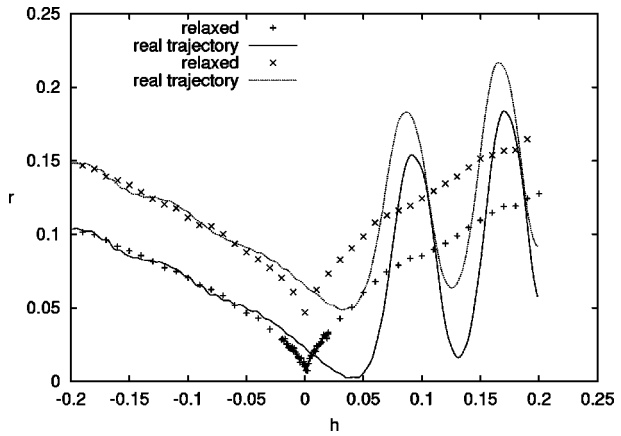

FIG. 1. The measured trajectory in the (r,h) plane for two different initial temperatures (solid lines). The crosses show the reduced equilibrium temperature $r(h)$ corresponding to energy density $\epsilon(h)$. The size of the system was $L=64$, and the inverse rate of change of h is $a=100$.

effects in the motion of modes with different $\hat{\mathbf{k}}$ and apparently related to the presence of an h-dependent common effective mass.

After careful testing of the simplified procedures against the conceptually better founded methods in equilibrium we decided to use algorithm 5 throughout this paper.

Although the different algorithms were normalized to yield equal masses in equilibrium, it is not obvious that they will agree also for a nonequilibrium crossover connecting two points of the (r,h) plane. We shall return to the comparison of the nonequilibrium results obtained with different methods at the end of Sec. IV.

III. PASSING BY THE CRITICAL POINT

We have solved Eq. (3), the discretized version of Eq. (1), numerically. A starting configuration was thermalized in the presence of the initial magnetic field $(h_0=-0.2)$, in such a way that a predefined value of the average kinetic energy density was reached. This thermal state was taken for the initial configuration when solving the field equation with an external magnetic field tuned with constant velocity dh/dt. With the parameters we used the correlation length of the initial configuration was approximately equal to one lattice unit.

In the present investigation the same range of the parameters $r,dh/dt$ was covered as in [7]. For each value of $r,L,a\equiv(dh/dt)^{-1}$ runs with ~ 20 different equilibrium configurations were averaged.

An approximate idea of the part of the Ising phase diagram explored in our numerical investigation can be given by drawing the measured (r,h) trajectories for different values of $r_{initial}$ and a (see Fig. 1).

Due to the time dependence of the external force $h(t)$ the full energy density $\epsilon(t)$ is not conserved; we shall parametrize it as $\epsilon(h)$. In principle, it might depend on the parameter a too, but for the range investigated in this paper we did not experience any a dependence of the energy density. The reduced (Ising) temperature, which is defined through the average kinetic energy per site, slowly drops in the first part of the crossover. However, having passed by the critical point $(h=0,r=0)$ a deterministic oscillation in r starts, which survives the averaging over the ensemble of initial thermal configurations. For comparison we have also displayed in Fig. 1 the reduced temperatures corresponding to the equilibrium states belonging to the different values of the energy density $\epsilon(h)$. The latter was determined by stopping the variation of h at a certain value h_{stop}, and then relaxing the system with fixed $h=h_{stop}$ (and hence with conserved energy) to equilibrium. After the thermalization of this state was complete, we measured its equilibrium temperature. These runs were performed for every nonequilibrium trajectory for 40 equidistant intermediate values of $h_{stop}\in(-0.2,0.2)$.

Figure 1 clearly shows how the system slows out of equilibrium. As the critical point is approached, the thermalization time scale grows above the time scale $(\sim ha)$ of moving in the phase diagram. Thus, in the second part of the crossover two effects seem to be present. First, the spectral density of the configuration corresponds to the equilibrium at an earlier h value—this means an overcooling in QCD language. Second, the low-$\mathbf{k}$ modes become highly excited and begin to oscillate with a frequency determined by the effective mass scale. The oscillation is synchronously present in the entire spectrum, i.e. the kinetic energy of each ''well-behaving'' $(\hat{k}^2>1)$ mode oscillates coherently. The oscillation is not due to any direct strong coupling between the modes, but is driven by the oscillation of the homogeneous mode $(\bar{\Phi})$ (see Fig. 2(a)). The UV modes adiabatically follow the slow oscillation of the order parameter (see Fig. 2(b)), which enters parametrically through a common effective mass in the corresponding equation of each mode.

One may define the error of the OP trajectories from different thermal initial conditions as the standard dispersion of the OP(t) values at fixed t. This error comes out at ≈ 0.007 for $h<0$ and ≈ 0.02 for $h>0$, which is about 100 times smaller than the amplitude of the oscillations.

For comparison the equilibrium OP values are also displayed in Fig. 2(a). These values come from thermal solutions of Eq. (1) with the (r,h) values chosen from the equilibrium points of Fig. 1.

The OP evolution displayed in Fig. 2(a) is by itself a challenge seeking quantitative interpretation. We shall elaborate on it in detail in Sec. IV.

IV. HOW LARGE DOES THE CORRELATION LENGTH GROW?

The main physical motivation of our investigation was to answer the question in the title of this Section. We have used the fast method described in Sec. II for deducing the actual nonequilibrium value of the correlation length, that is, the inverse σ mass.

In Fig. 3(a) we display the h history of the correlation length obtained on a 64^3 lattice with an initial reduced (Ising) temperature $r_i=0.083$ for four values of the a param-

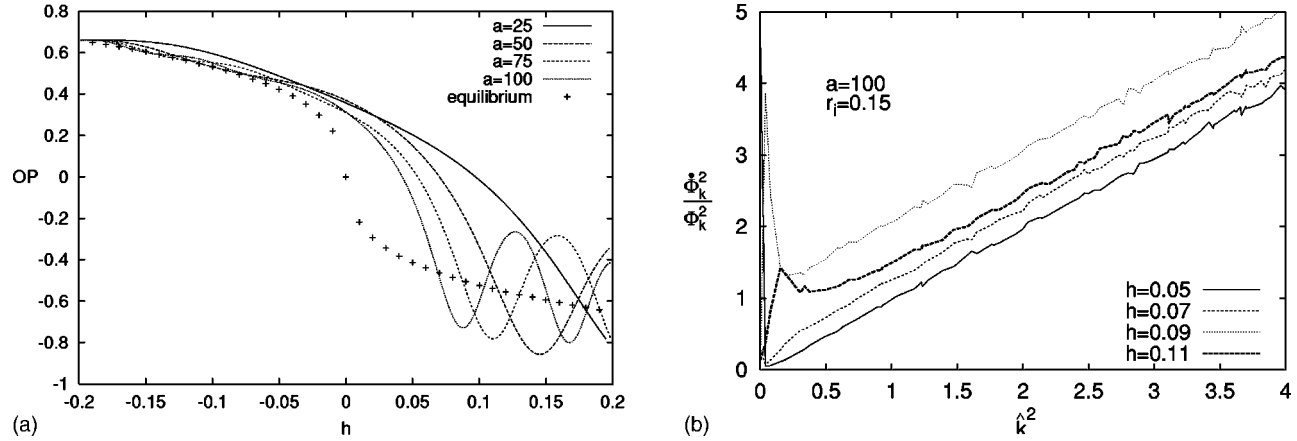

FIG. 2. (a) OP trajectories for different $dh/dt=a^{-1}$ values ($L=64$, $r_{initial}=0.15$). The equilibrium $\bar{\Phi}(h)$ curve is represented by crosses. (b) Temporal variation of the left hand side of Eq. (9) synchronized by the OP oscillation.

eter. The (r,h) trajectory starting from this r_i passes the closest by the critical end point ($r_{min}=0.007$); see the lower curve in Fig. 1. Again, the equilibrium correlation length values obtained from analyzing long thermal time evolutions with an identical method are displayed in the same plot.

When compared with the estimate of [7] the most dramatic difference is obvious: even the slowest variation of h considered by BR is in reality much too strong. The critical slowing down of the internal interactions pushes the system far out of the equilibrium state corresponding to the actual magnetic field value. This is the reason that after passing the maximum of the correlation length, reached with the expected ''supercooling'' in h, ξ starts to oscillate and the correlation length very steeply drops to a minimum. This oscillation has opposite ''phase'' if compared to the (Ising) temperature. A probable explanation for this phenomenon is that a shrinking correlation length means larger σ mass and hence an increase in the frequency of the microscopic oscillations of the UV modes. The energy of a weakly coupled UV mode—such as of a tuned linear oscillator—gets larger with an increase of its frequency.

The qualitative picture is the same in a wider neighborhood of the critical end point as one can see from Fig. 3(b), which corresponds to a trajectory passing somewhat farther away ($r_i=0.15$; the upper curve in Fig. 1).

The period of the oscillation in QCD temperature based on the T_{QCD}-h correspondence proposed in [7] seems to be much smaller than the spread of the freeze-out temperature estimates appearing in the literature. Therefore our main qualitative result is that the expected increase in the coherence of the pion radiation might be missed if the actual freeze-out happens at a temperature slightly beyond the maximum of the correlation length. Ideally, accurate measurements of the freeze-out temperatures of different meson species coupled to σ might allow one to map out the variation of its correlation length across the hypersurfaces of the respective ''last scatterings'' as predicted by our analysis.

One can compare the exact nonequilibrium $\xi(h,a)$ function to the estimate of BR in more quantitative detail. The maximal values of the correlation length in units of the initial ξ_0 are in the range $(2.5–3.5)\xi_0$. The amount of supercooling is generically larger from the numerical solution of the Φ^4 dynamics, in comparison to the result of the first order dynamics conjectured in [7].

A good measure of the amount of physical supercooling as a function of the h velocity is offered by the shift in the

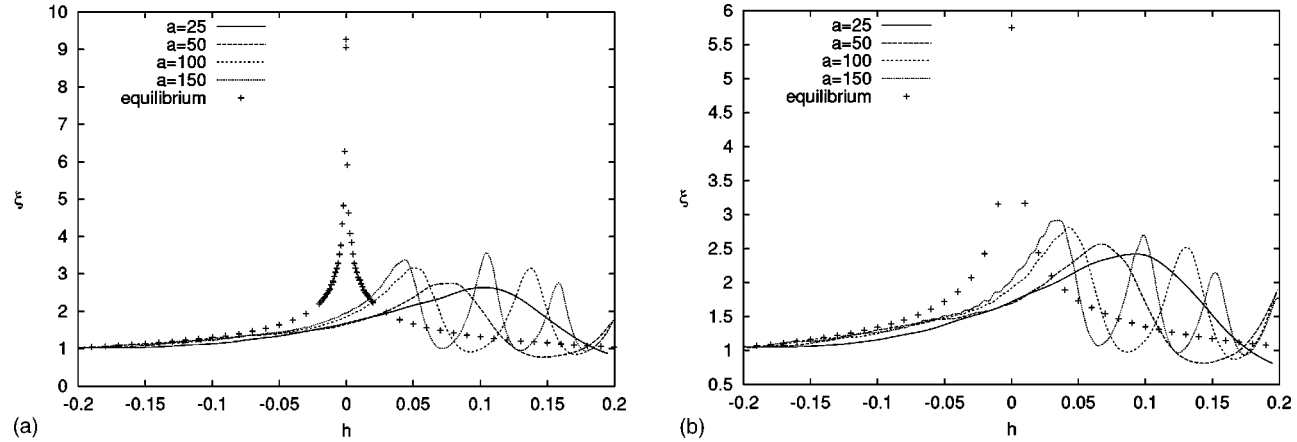

FIG. 3. Evolution of correlation length during a crossover compared to the equilibrium values along the (r,h) route depicted in Fig. 1. ($L=64, r_{i,a)}=0.083, r_{i,b)}=0.15$.) Crosses give the results of equilibrium measurements.

location of the first maximum of the correlation length, $h(\xi_{max})$. This value turns out to scale with the velocity of the h variation:

$$h(\xi_{max},a)=ca^{-0.5\pm0.01}. \tag{11}$$

The values of ξ_{max} themselves also follow a scaling form as suggested in [7] on the basis of dynamical scaling considerations. We find numerically

$$\xi_{max}(a)=c'a^{0.211\pm0.01}. \tag{12}$$

The value of this exponent agrees with the prediction of BR, when it is applied to class A. Then their prediction for the exponent yields $\nu/\beta\delta/(1+z\nu/\beta\delta)=0.222$, with $\nu=0.630$, $\beta=0.326$, $\delta=4.8$ and $z=2+[6\ln(4/3)-1]\eta, \eta=0.0335$ [6]. When the initial (Ising) temperature is tuned to approach the critical point within 2–3 % from above, it turns out that the form of the $\xi(h)$ function remains qualitatively the same as described above. The ξ values at the first maximum are about four times larger than those taken in the first minimum following them.

The second maximum of ξ appearing in our numerical solution very probably cannot be observed experimentally, since the fireball breaks up into noninteracting mesons before reaching the corresponding low temperature.

The sensitivity of the results to the size of the system is also an important issue, since at present the linear size of the plasma droplet is estimated to be about $6\xi_0$. Since we have chosen ξ_0 for the lattice constant, one might expect to reach the maximal allowed correlation length in a much smaller lattice volume. We have tested the robustness of the above conclusions by varying the lattice size between 16 and 64. No important variation was seen when changing the size from $L=64$ down to $L=32$, but a 20% drop in the maximum of ξ appears when going down to $L=16$.

The lattice we used in this investigation is rather coarse ($|m|a_x=1$). The idea behind this choice is that we work near the critical point, in the scaling regime. At equilibrium when the correlation length grows very large it is obvious that the actual value of the lattice spacing cannot matter. However, actually a factor of 3–5 increase was experienced ''only,'' so we have to check that the *dynamical* scaling hypothesis

$$\xi(r,h,t)=\lambda^{\nu}\xi(\lambda r,\lambda^{\nu/\mu}h,\lambda^{-\nu z}t),$$

$$\overline{\Phi}(r,h,t)=\lambda^{-\beta}\overline{\Phi}(\lambda r,\lambda^{\beta\delta}h,\lambda^{-\nu z}t) \tag{13}$$

is satisfied by the solution of Eq. (1). The observed dynamical scaling behavior of ξ_{max} and $h(\xi_{max})$ already suggests that our system evolves in the scaling regime. As a direct proof for this, we have rescaled the reduced temperature, the magnetic field and the $a=dt/dh$ parameter in such a way that we could expect a factor of 2 increase in the correlation length if the first equation of Eq. (13) is obeyed. The field Φ has been rescaled as dictated by the second equation. From the rescaled equations the evolution of the order parameter and of the inverse correlation length has been extracted. Before the oscillation sets in the agreement with the expectations based on the scaling hypothesis is very convincing. It improves as the system approaches the critical point. This is a clean argument for the independence of our results of the lattice spacing. This conclusion is certainly true until the first maximum of the correlation length is reached. For the oscillatory motion a second order dynamics is relevant; therefore the scaling behavior based on $z\approx2$ should be violated.

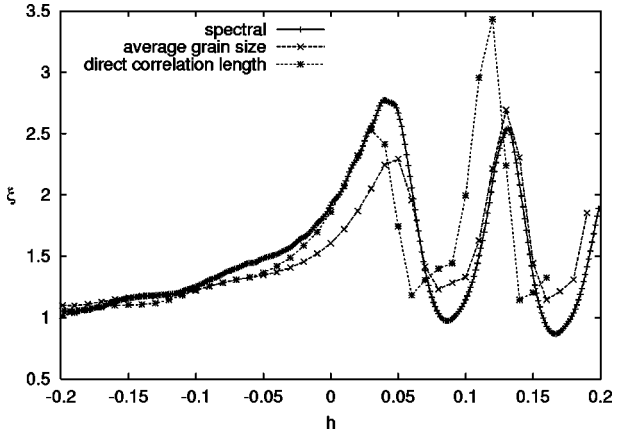

FIG. 4. Comparison of the time dependence of the correlation lengths determined by three different methods: the ''direct'' correlation length, the average grain size and the inverse mass determined with spectral algorithms. Shown is the evolution during the nonthermal crossover passing close to the Ising critical end point. ($L=32, r_i=0.15, a=100$; for definitions see the text.)

The final question to be discussed in this section is to what extent the observed features of the time dependence of ξ depend on the algorithm used for its determination. In Fig. 4 a typical time evolution is displayed for the three characteristic lengths introduced in Sec. II. Using the $m_{eff}=g_i(\xi_i)$ relations determined in equilibrium we see very good agreement of all three before the system is slowed out of equilibrium. Next all three enter an oscillatory regime, with about the same amplitude, but with a certain ''phase shift.''

This observation makes it more difficult to relate the location of the first maximum in h to the freeze-out temperature. One has to work with that length which is coupled to the microscopic mechanism producing a certain observable. For example, the high frequency part of the σ field is probably well represented by a gas of particles with the effective frequency determined by the ''susceptibility dispersion'' method 5 of Sec. II. The decay products of these hard particles will reflect this frequency. The softest part of the pion spectra probably comes from the coherent decay of the longest wavelength components of the field configuration; therefore a characteristic coherence length closer to the ''grain size'' (method 2) will be followed.

V. THE EFFECTIVE ORDER PARAMETER DYNAMICS

In statistical physics noisy first order effective equations are used for the longest wavelength hydrodynamical modes to describe relaxation phenomena. These equations have to be written down for the order parameter fields and also for composite objects which correspond to densities of conserved quantities [6]. From this viewpoint it is not clear what

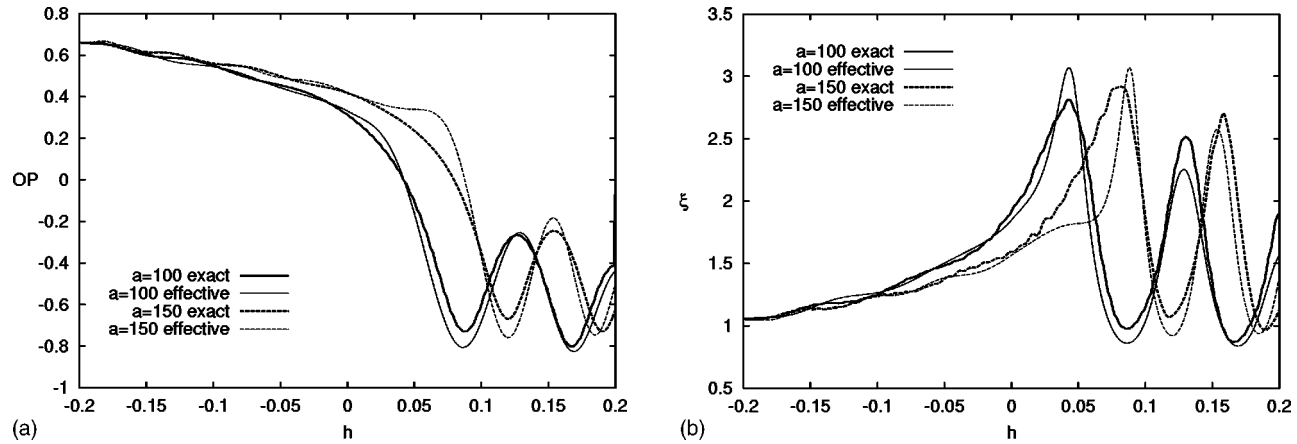

FIG. 5. (a) Exact evolution of the OP and the solution of Eq. (14) for two values of a. (b) Exact evolution of the correlation length and its values estimated with the help of the effective OP trajectory (see text) for two values of a. ($L=64, r_i=0.15$.)

could be the foundation for the proposal of BR to write down directly an equation for the relaxation of the inverse correlation length.

We follow the more conventional path and discuss first the effective dynamics of the order parameter. After presenting considerable evidence for the validity of our approach to the OP, we shall also be able to build upon it a quite natural interpretation of the observed behavior of the correlation length.

It is obvious that one cannot account for the oscillatory behavior of the order parameter experienced after passing near the critical end point by just using a first order effective dynamics. This means that our system actually leaves the hydrodynamical regime. Therefore, we propose to complete the effective OP equation with an ''acceleration'' term. For the effective free energy we use the simplest quadratic form, which corresponds to an oscillator potential centered at the equilibrium value of the order parameter [8]. We emphasize that no noise is introduced.

The proposed linear equation is of the form

$$a^{-2}\ddot{\overline{\Phi}}(h)+a^{-1}\Gamma(h')\dot{\overline{\Phi}}(h)+m_{eq}^2(h')[\overline{\Phi}(h)-\overline{\Phi}_{eq}(h')]=0. \tag{14}$$

In this fully deterministic equation an overdot means derivation with respect to h. In view of the relation $h=at$, the derivatives originally refer to the time. The determination of the h-dependent coefficients $m_{eq}=\xi_{eq}^{-1}, \overline{\Phi}_{eq}$ follows the methods described in previous sections. However, their values are taken not at the actual h, but at a somewhat smaller value h', which corresponds to an earlier equilibrium state. This is the simplest way to incorporate the ''slowing out of equilibrium'' phenomenon into the proposed equation.

The shift $h-h'$ is established by optimizing the agreement with the measured order parameter trajectory. Three physical pictures for this shift were tested and benchmarked by the mean-square (MS) deviation of the reconstructed OP trajectory from the measured one (δ^2). In the first one a global delay parameter is introduced which acts with equal strength before and after reaching the neighborhood of the critical point ($\delta^2=0.0034$). In the second version one switches on the h delay only when $h\geqslant 0$ ($\delta^2=0.094$). In the third version the delay grows linearly from 0 to a final value that was fitted to the data. This last method produced the smallest MS deviation ($\delta^2=0.0029$); therefore below we shall present results obtained with this method. The representative δ^2 values refer to a 32^3 lattice with $r_i=0.15, a=100$. As expected the fitted slope of the linear shift, $h-h'=\text{const}\times(h-h_0)$, clearly increases as r_i gets smaller. The value of the constant coefficient changes monotonically from 0.02 to 0.1 while r_i varies from 0.2 to 0.1.

The reconstruction of the measured OP trajectory turned out to be rather insensitive to the value of the relaxation rate $\Gamma(h')$. Furthermore, no h' dependence could be observed. In the wide range $\Gamma=0.01$–0.6, an acceptable agreement of the real and the reconstructed OP trajectories was found.

A nonperturbative, near equilibrium determination of Γ was attempted by stopping h at a certain value h_{stop} and fitting the relaxation of $\overline{\Phi}$ toward equilibrium to an exponential rate. The estimate for Γ was found to be in the range 0.005–0.025, independently of r_i and a. In a model investigated previously we found that during the equilibration the relaxation rate approaches its perturbative value strictly from below [11].

Equation (14) was solved with the initial values for the OP deduced from the full system: $\overline{\Phi}(h=-0.2), \dot{\overline{\Phi}}(h=-0.2)$. OP trajectories resulting from different realizations of the initial thermal ensemble give slightly different initial conditions for Eq. (14). This uncertainty sets the error of the reconstructed trajectory. [The average variance of the solution of Eq. (14) is $\sigma_{th}^2\approx 0.0001$ for $h<0$ and $\sigma_{th}^2\approx 0.0006$ for $h>0$.]

In Fig. 5(a) we compare the true and the reconstructed OP trajectories. The quality of the agreement fluctuates somewhat, but its δ^2 value is less than 0.02 in the whole $L,T,a\geqslant 50$ region, considered in this paper. In principle one could attempt to further improve the analytic interpretation of the OP dynamics by introducing a memory kernel into the equation for $\overline{\Phi}$, but we believe that our proposed equation captures the essence of the actual OP dynamics.

With this achievement, we can return to the discussion of the nontrivial variation of the correlation length. We build our description on our understanding of the order parameter dynamics.

The evolution of the system is investigated in the close neighborhood of the critical point, in the so called scaling regime. In equilibrium, by choosing the scale factor $\lambda = 1/r$ in Eq. (13) one finds the usual form of the scaling behavior of the correlation length and of the order parameter. In Fig. 1 we have shown the trajectory $r = r(h)$ of the evolution of the system for $t = ah$. If this trajectory is simple enough, as in the left part of Fig. 1, a unique $r(\xi)$ function can be extracted, for instance, from the first relation, and after its substitution into the second a functional relation $\xi(\bar{\Phi})$ is obtained. One may then deduce the piecewise unique function $d\bar{\Phi}(\xi)/d\xi$, which can be used to rewrite the effective equation for $\bar{\Phi}$ [Eq. 14)] into an equation for $\xi(h)$.

Motivated by this argument, we have plotted $\xi(t)$ against $\bar{\Phi}(t)$, both measured during the actual real time evolution of the system. It turns out that a unique functional relation $\xi(\bar{\Phi})$ can be recognized in the regime of monotonic OP evolution (cf. Fig. 2(a)). In the oscillatory OP regime first one has to average the $\xi = m_{eff}^{-1}$ values taken at different passes through $\bar{\Phi}$. The function $\xi(\bar{\Phi})$ is extracted only after this step. A very good fit valid for the whole evolution period of the form

$$\xi^{-2} = c\bar{\Phi}^q + p, \quad q \approx 2.3, \quad c \approx 2 \tag{15}$$

was obtained, with the parameter p slightly depending on the velocity of the h variation. The agreement of the measured $\xi(h)$ function with the one reconstructed by mapping the computed time evolution of the OP using the above relation is quite spectacular (see Fig. 5(b)).

We conclude this section by discussing a more ''theoretical'' approach to the determination of Γ, m_{eq} and Φ_{eq}, by observing that these quantities refer to (near) equilibrium situations. In our very simple model their nonperturbative values were easily determined from the microscopic data. In the case of more realistic models, however, one may attempt to use perturbative estimates for the masses, the damping rates and the equilibrium order parameter. We have also tested the quality of the reconstructed OP trajectory in the present model when these coefficients were taken from perturbation theory.

As is well known even a resummed perturbation theory fails in the vicinity of the critical temperature due to its bad behavior in the IR regime. The divergence of the correlation length and as a consequence also of the effective expansion parameter $\lambda T \xi$ (see for example [12]) excludes its use in the scaling regime. In a finite system, however, with an IR cutoff L we could attempt to extract the equilibrium mass, the equilibrium OP value and the damping rate of the OP using two-loop lattice perturbation theory. The mass comes from the second derivative of the effective potential at the minimum, the OP is the location of this minimum, and for the damping rate we use the formula derived in [13]. The two-loop perturbative effective potential was computed with self-consistent propagators on a finite lattice and we extracted from it the position of the minimum and the second derivative in this point along the (r,h) route shown in Fig. 1. The mass used in the propagators was determined from a one-loop gap equation.

The expression for the two-loop effective potential on a lattice is

$$\begin{aligned} V_{2\,loop}(\bar{\Phi}) &= V_{tree}(\bar{\Phi}) + \frac{T}{L^3}\sum_{\mathbf{k}} \log\frac{\omega(\hat{\mathbf{k}},\mu)}{T} \\ &\quad - \frac{\lambda T^2}{8L^6}\left[\sum_{\mathbf{k}} \frac{1}{\omega^2(\hat{\mathbf{k}},\mu)}\right]^2 \\ &\quad - \frac{\lambda \bar{\Phi}^2 T^2}{12L^6}\sum_{\mathbf{k}}\sum_{\mathbf{p}}\sum_{\mathbf{q}} \frac{\delta^{(3)}(\hat{\mathbf{k}}+\hat{\mathbf{p}}+\hat{\mathbf{q}})}{\omega^2(\hat{\mathbf{k}},\mu)\omega^2(\hat{\mathbf{p}},\mu)\omega^2(\hat{\mathbf{q}},\mu)}, \end{aligned} \tag{16}$$

where $\omega^2(\hat{\mathbf{k}},\mu) = \hat{\mathbf{k}}^2 + \mu^2$. The mass was determined from the one-loop gap equation

$$\mu^2 = m^2 + \frac{\lambda}{2}\bar{\Phi}^2 + \frac{\lambda T}{2L^3}\sum_{\mathbf{k}} \frac{1}{\omega^2(\hat{\mathbf{k}},\mu)}. \tag{17}$$

In view of Eq. (2) we put $\lambda = 6$.

The inaccuracy of the two-loop perturbation theory comes overwhelmingly from the fact that for the lattice spacing considered in this paper the estimate of the critical temperature exceeds the value numerically determined by us at $|m|a_x = 1$ by 25%. Repeating both the numerical and the perturbative calculation with $|m|a_x = 0.5$, the deviation diminishes to 5%. Despite all inaccuracies of the perturbation theory the solution of Eq. (14) based on the perturbative potential $V_{2\,loop}$ turns out to follow the real trajectory quite closely, although because of the ill-determined OP values the deviation also has a systematic error ($\delta^2 \approx 0.014$).

For an alternative estimate of $\xi_{eq}(h)$ we used Widom's scaling form [14] as was done by BR. This yields $\xi_{eq}(h)$ values close to the measured equilibrium correlation length. The solution of Eq. (14) fitted to the measured curve with this coefficient is of only slightly lower quality than the fully nonperturbatively reconstructed one ($\delta^2 \approx 0.0061$).

VI. CONCLUSIONS

In this paper we have presented a detailed discussion of the real time nonequilibrium evolution of the classical Φ^4 field theory when it passes near the critical end point in its (r,h) phase diagram under the influence of a time dependent external magnetic field. The numerical investigation was focused on the variation of the correlation length. A quick but accurate method for determination of the instant nonequilibrium mass of the Φ field was employed, relying on the para-

metrical relation of the spatial domain of coherence of field fluctuations to the mass.

For a wide range of the rate of variation of the magnetic field we experienced a slowing of the system out of the hydrodynamical regime. This phenomenon was demonstrated in the behavior of all quantities used for the characterization of the system: the average kinetic energy per site, the order parameter and the correlation length all showed oscillations when the value of the external magnetic field moved beyond the point of ''supercooling.''

A simple effective equation was shown to describe this dramatic feature of the OP evolution. The coefficients of the second order differential equation written down for the order parameter take their values from equilibrium. They can be determined from separate simulations, but perturbative estimates also led to reasonable description of the OP evolution. A more important feature of the effective equation is that the coefficient functions should be computed for values of the external magnetic field corresponding to some earlier stage of the evolution. The gradual increase in this shift reflects the cumulative effect of the critical slowing down in the proposed effective description.

The motivation for this investigation came from its possible relevance to σ-meson dynamics in high energy heavy ion collisions [1]. The weakest point in taking the above features over into QCD is the lack of a quantitatively accurate mapping between QCD and the Φ^4 model in the (T,μ) plane. Still, our results can be compared in a useful way with the scenario put forward in [7] for the evolution near a hypothetical critical QCD end point.

In the context of heavy ion collisions, it would be interesting to see the effect of a coherently oscillating long wavelength σ background with variable correlation length on transversal jet quenching.

ACKNOWLEDGMENTS

The authors gratefully acknowledge important discussions with A. Jakovác and G. Veres.

[1] M. Stephanov, K. Rajagopal, and E. Shuryak, Phys. Rev. Lett. **81**, 4816 (1998).
[2] For a recent review, see F. Karsch, Talk at QM2001, Stony Brook, 2001, BI-TP-2001-06.
[3] A. Barducci, R. Casalbuoni, S. de Curtis, R. Gatto, and G. Pettini, Phys. Lett. B **231**, 463 (1989); A. Barducci, R. Casalbuoni, G. Pettini, and R. Gatto, Phys. Rev. D **49**, 426 (1994).
[4] Z. Fodor and S.D. Katz, ''Lattice Determination of the Critical Point of QCD at Finite T and μ,'' hep-lat/0106002.
[5] M. Stephanov, K. Rajagopal, and E. Shuryak, Phys. Rev. D **60**, 114028 (1999).
[6] P.C. Hohenberg and B.I. Halperin, Rev. Mod. Phys. **49**, 435 (1977).
[7] B. Berdnikov and K. Rajagopal, Phys. Rev. D **61**, 105017 (2000).
[8] Sz. Borsányi, A. Patkós, J. Polónyi, and Zs. Szép, Phys. Rev. D **62**, 085013 (2000).
[9] For an analogous application, see K. Rajagopal and F. Wilczek, Nucl. Phys. **B399**, 395 (1993).
[10] W.H. Tang and J. Smit, Nucl. Phys. **B510**, 401 (1998).
[11] Sz. Borsányi and Zs. Szép, Phys. Lett. B **508**, 109 (2001).
[12] M. Pietroni, Phys. Rev. Lett. **81**, 2424 (1998); Talk given at the 5th International Workshop ''Thermal Field Theories and their Applications,'' 1998, Regensburg, Germany, hep-ph/9809390.
[13] S. Jeon, Phys. Rev. D **52**, 3591 (1995); E. Wang and U. Heinz, *ibid.* **53**, 899 (1996); G. Aarts and J. Smit, Phys. Lett. B **393**, 395 (1997); W. Buchmüller and A. Jakovác, *ibid.* **407**, 39 (1997).
[14] E. Brézin, J.C. Le Guillou, and J. Zinn-Justin, in *Phase Transitions and Critical Phenomena*, edited by C. Domb and M.S. Green (Academic Press, New York, 1976), Vol. 6.